Neuron, Volume 64

Supplemental Data

DSCAM and DSCAML1 Function in Self-Avoidance in Multiple Cell Types in the Developing Mouse Retina

Peter G. Fuerst, Freyja Bruce, Miao Tian, Wei Wei, Justin Elstrott, Marla B. Feller, Lynda Erskine, Joshua H. Singer, and Robert W. Burgess

Supplemental Figure 1. A null allele of *Dscaml1*. **A**, Cartoon of DSCAM and DSCAML1 conserved protein domain structure. Both genes encode ten immunoglobulin (Ig) and six fibronectin (FN) domains, a transmembrane domain and cytoplasmic domain terminating in an identical PDZ binding motif. **B**, An ES cell line containing a gene trap inserted within the third, 210 kb, intron of *Dscaml1* was acquired from the Sanger Centre and used to generate chimeric mice. **C**, Northern blot analysis of mRNA isolated from the brains of wild type, *Dscaml1*$^{GT/+}$ and *Dscaml1*$^{GT/GT}$ mice (N=3, two shown). A 7 kb band, corresponding to full length *Dscaml1*, was detected in the wild type and *Dscaml1*$^{GT/+}$samples, while no full length *Dscaml1* was detected in mRNA samples prepared from *Dscaml1*$^{GT/GT}$ brains. A truncated product corresponding to a fusion of the 5' end of *Dscaml1* with LacZ was detected in mRNA samples prepared from *Dscaml1*$^{GT/+}$ and *Dscaml1*$^{GT/GT}$ brains. The probe used was cDNA contained in exons 1-3 of *Dscaml1*, upstream of the gene trap insertion site and designed to detect the truncated transcript. **D-G**, β-gal reporter activity was assayed in retinal sections at postnatal day (P) 6, 12 and 30. At P12 β-gal activity was detected in the soma of cells in the amacrine and bipolar containing portion of the INL, as well as in the IPL. By P30 β-gal activity was no longer detected in the bipolar containing portion of the INL but was

localized to the photoreceptors (pr) and OPL, as well as cells in the amacrine containing portion of the INL. **H**, No β-gal activity was detected in wild type controls. The scale bars below the panels are equivalent to 200

μm.

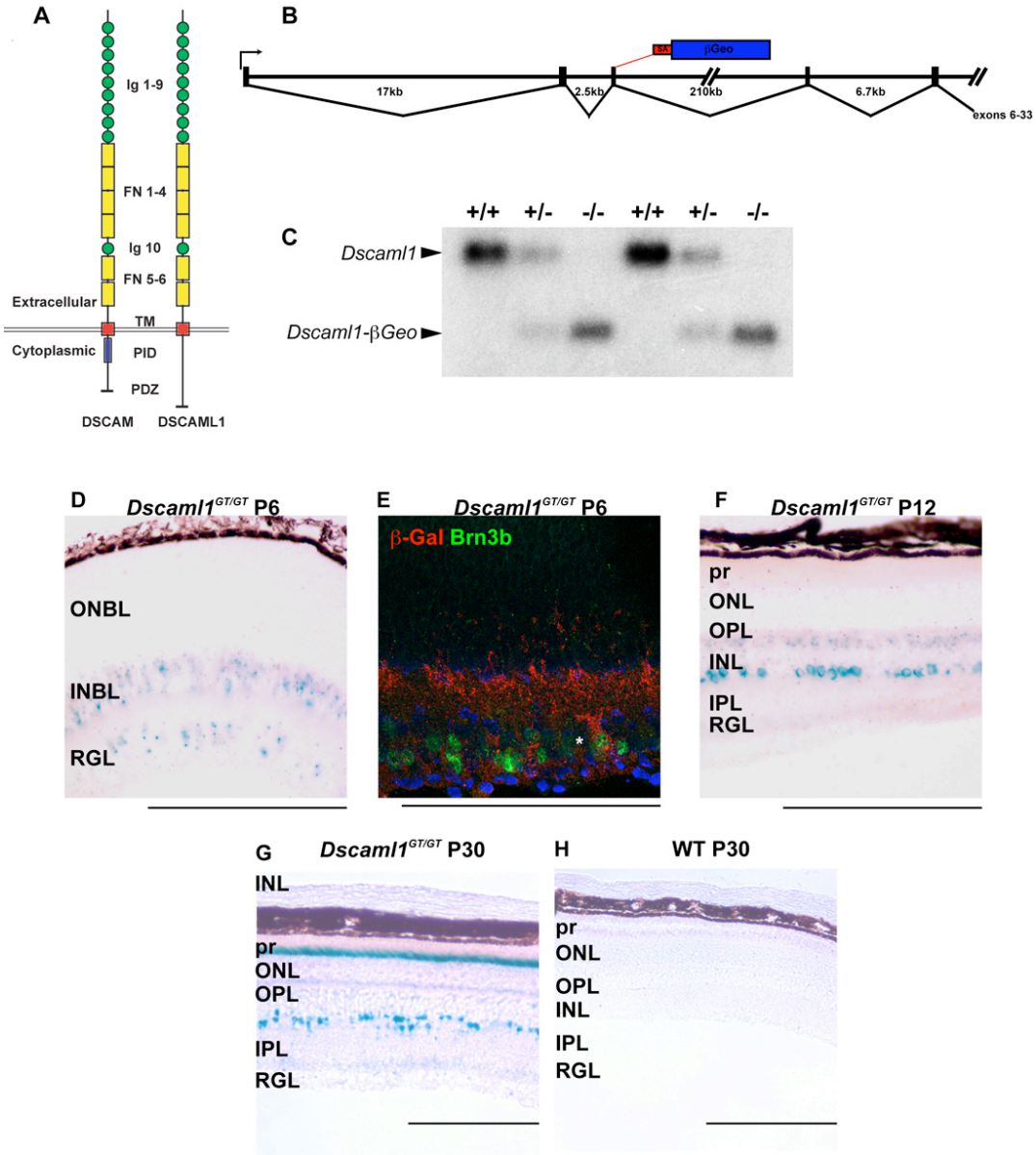

Supplemental Figure 2. Expression of *Dscaml1* in the brain. *Dscaml1*$^{GT/+}$ and *Dscaml1*$^{GT/GT}$ brains were cut into 50 μm coronal sections using a vibratome and stained for β-gal activity to monitor *Dscaml1* expression. **A**, **B**, β-gal activity stained the superior colliculus strongly. Two distinct laminae contain *Dscaml1*-positive cells, which are more abundant and disorganized in the *Dscaml1*$^{GT/GT}$ brain. **C**, **D**, *Dscaml1* expression was observed in CA3 region of the hippocampus, as well as the granual cell layer of the dentate gyrus (DG-sg) and the hippocampal formation (HPF), the latter contained an increase in *Dscaml1*-positive cell in the *Dscaml1*$^{GT/GT}$ brain. **E**, **F**, Strong *Dscaml1* expression was observed in the piriform cortex (PIR) and amygdala. **G**, **H**, *Dscaml1* expression was observed in a subset of cells within the caudate putamen. These cells were aggregated in the *Dscaml1*$^{GT/GT}$ brain (arrows) compared to *Dscaml1*$^{GT/+}$. The scale bar in (**H**) is equivalent to 1.45 mm in **A**, **B**, **E**, **F**, **G** and **H**, and 1 mm in **C** and **D**.

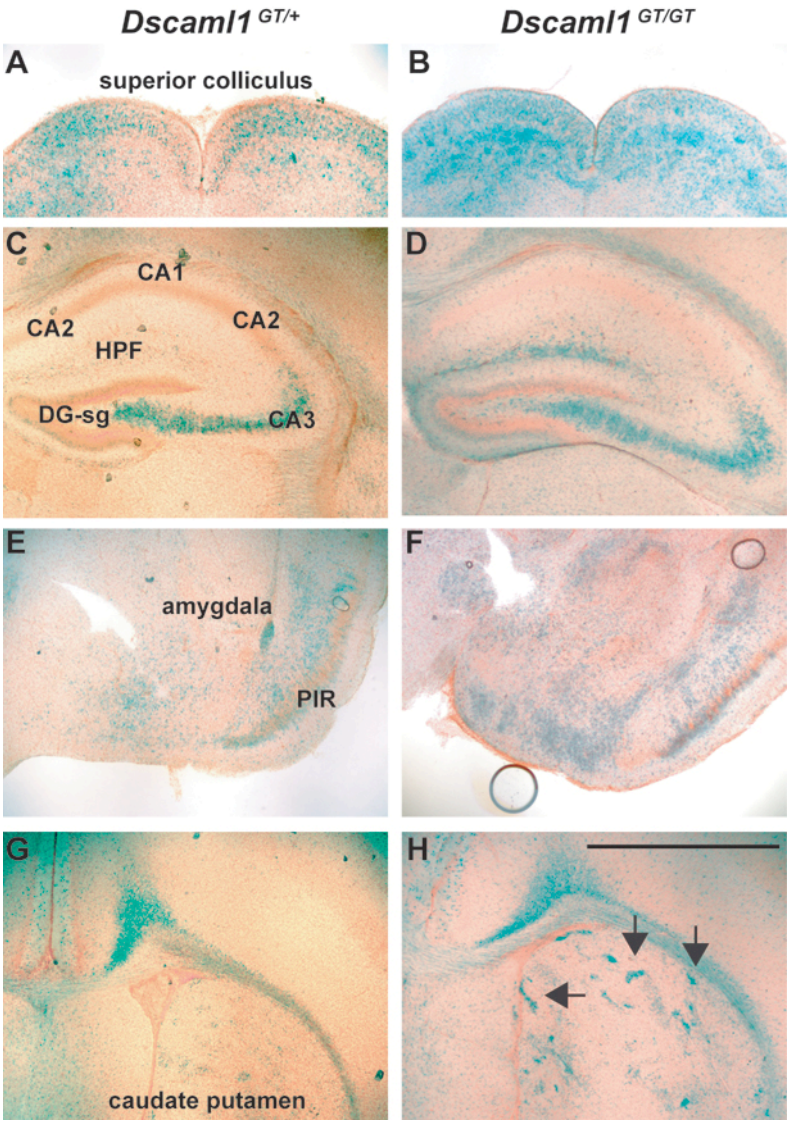
Dscaml1 GT/+
Dscaml1 GT/GT
A
superior colliculus
B
C
CA1
CA2
CA2
HPF
DG-sg
CA3
D
E
amygdala
PIR
F
G
caudate putamen
H

Supplemental Figure 3. *Dscaml1* is not expressed in cholinergic amacrine cells, SYT2-positive cone bipolar cells or cones. **A**, *Dscaml1*$^{GT/GT}$ retina stained with antibodies to ChAT and β-gal. **B**, *Dscaml1*$^{GT/GT}$ retina stained with antibodies to SYT2 and β-gal. **C**, Section of *Dscaml1*$^{GT/GT}$ retina showing photoreceptor outer segments stained with antibodies to β-gal and peanut lecithin (PNL), a marker of cones. Colocalization of cell type markers and β-gal was not observed. The scale bar in (C) is equivalent to 42 μm in A, 35.5 μm in B and 45.5 μm in C.

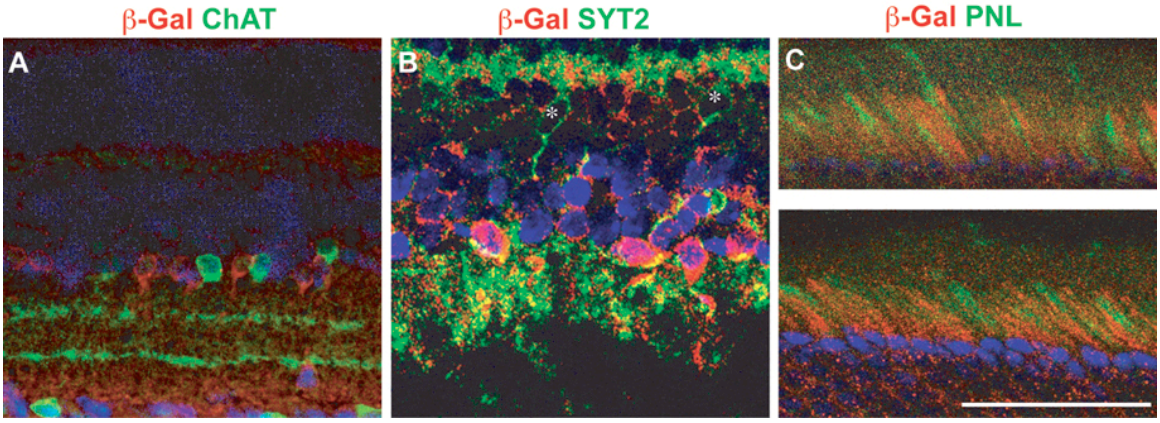

Supplemental Figure 4. Characterization of Mito-Y positive RGCs. **A** and **B**, Montages of whole *Dscam*$^{+/-}$ (+/-) and *Dscam*$^{-/-}$ (-/-) retinas carrying the Mito-Y transgene. A large number of Mito-Y positive RGCs are present in the dorsal portion of the retina (up), while a sparser population of Mito-Y positive RGCs are distributed throughout the rest of the retina. Mito-Y positive RGCs aggregate and fasciculate in the *Dscam*$^{-/-}$ retina. Density Recovery Profiling (DRP) analysis was performed to determine if Mito-Y-positive RGCs constitute a mosaic population, as evidenced by the presence of an exclusion zone. **C**, A weak exclusion zone was detected in the wild type and *Dscam*$^{+/-}$ retinas, based on the dip below average density at short distances from the reference cell (N=3 for each *Dscam*$^{+/-}$ shown in figure; the first bin was discarded to reflect the diameter of the cell soma). **D**, In contrast, the mosaic pattern of Mito-Y positive RGCs was lost in the *Dscam*$^{-/-}$ retina, and cells were aggregated as indicated by the higher than average density of cells at short distances in the mutant. Values in DRP measure in **C** and **D** are mean ± standard deviation. **E**, Retinal cross-sections were stained with antibodies to ChAT to label cholinergic amacrine cells and the laminae of the inner plexiform layer in which they stratify their processes. Mito-Y RGC dendrites co-stratified with the ON ChAT band and slightly medial to the innerplexiform layer with respect to the OFF ChAT band (shown in 8 representative images). **F**, Dye fills of individual Mito-Y positive RGCs. Both bistratified (N=8) and monostratified (N=6) dendritic arbors were observed, indicating that the Mito-Y transgene is labeling a heterogeneous population of RGCs consisting of at least three cell types based on morphology and laminar specificity of their dendrites. The scale bar in (**B**) is equivalent to 1.55 mm in **A** and **B**, 127.5 μm in **E** and 150 μm in **F**.

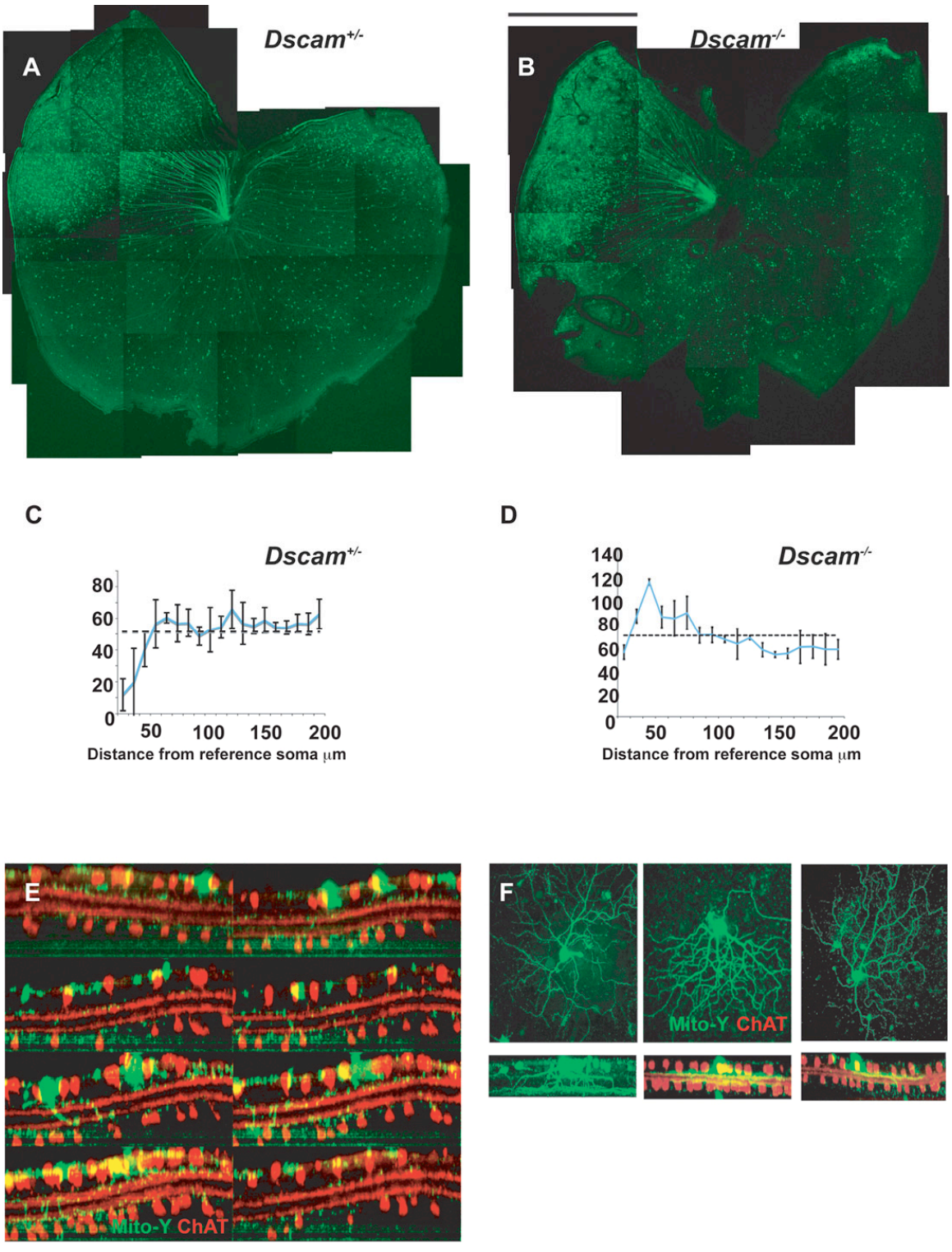
A
Dscam+/-
B
Dscam-/-
C
Dscam+/-
80
60
40
20
0
50
100
150
200
Distance from reference soma μm
D
Dscam-/-
140
120
100
80
60
40
20
0
50
100
150
200
Distance from reference soma μm
E
Mito-Y ChAT
F
Mito-Y ChAT

Supplemental Figure 5. Rod bipolar cells in the *Dscaml1*$^{GT/GT}$ retina. A, Section of retina stained with antibodies to PKCα, to detect rod bipolar cells and CTBP2. **B**, Rod bipolar cell dendrites stratify in the OPL, where the receive input from rods. The soma of rod bipolar cells is located in the scleral half of the INL. Rod bipolar cells project an axon through the IPL to the dyad synapse in the ON portion of the IPL. The letters at left denote the plane of section in C-J. **C-J**, Whole wild type and *Dscaml1*$^{GT/GT}$ retinas were stained with antibodies to PKCα and reconstructed in confocal Z-series. **C**, **D**, No difference was observed in the projection of distal dendrites when comparing wild type and *Dscaml1*$^{GT/GT}$ retinas. **E**, **F**, The proximal dendrites of rod bipolar cells were aggregated compared to wild type. **G**, **H**, No difference was observed in the somal spacing of rod bipolar cells in wild type and *Dscaml1*$^{GT/GT}$ retinas. **I**, **J**, Rod bipolar cell axonal terminals are more densely packed in the *Dscaml1*$^{GT/GT}$ retina compared to wild type, consistent with the increased cell number. The scale bar in (**J**) is equivalent to 63 μm **A**, 20.5 μm in **C**-**F**, 41 μm in **G** and **H** and 375.5 μm in **I** and **J**.

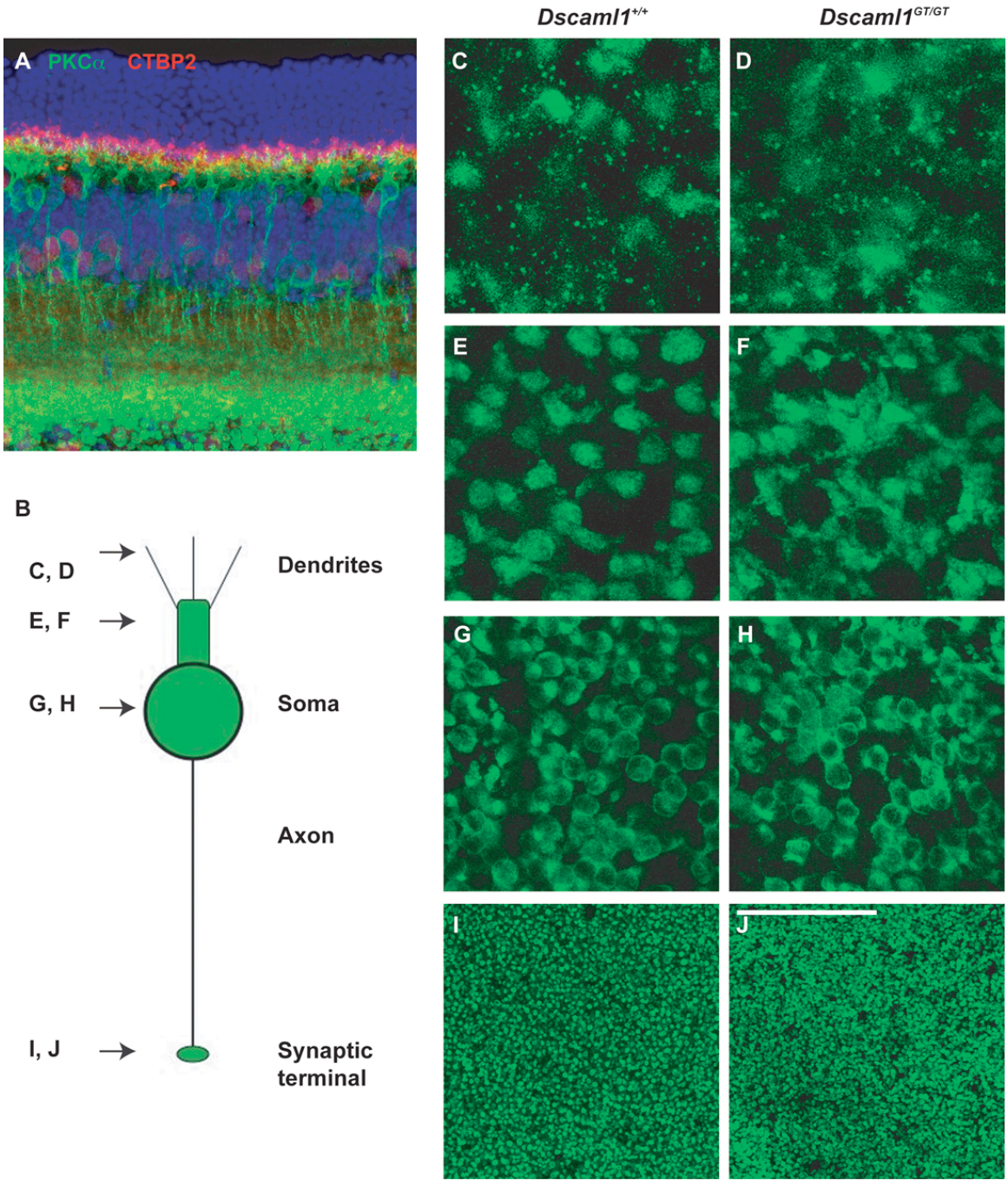
A PKCα CTBP2
B
C, D
E, F
G, H
I, J
Dendrites
Soma
Axon
Synaptic terminal
Dscaml1+/+
Dscaml1GT/GT
C
D
E
F
G
H
I
J

Supplemental Figure 6. TEM of wild type and *Dscaml1*$^{GT/GT}$ OPL at P9 and P15.

Transmission electron microscopy was used to examine the structure of the *Dscaml1*$^{GT/GT}$ outer plexiform layer (N=2 each). Fewer ribbon synapses were observed (arrows) in the *Dscaml1*$^{GT/GT}$ outer plexiform layer compared to wild type. The scale bar is equivalent to 7.5 μm.

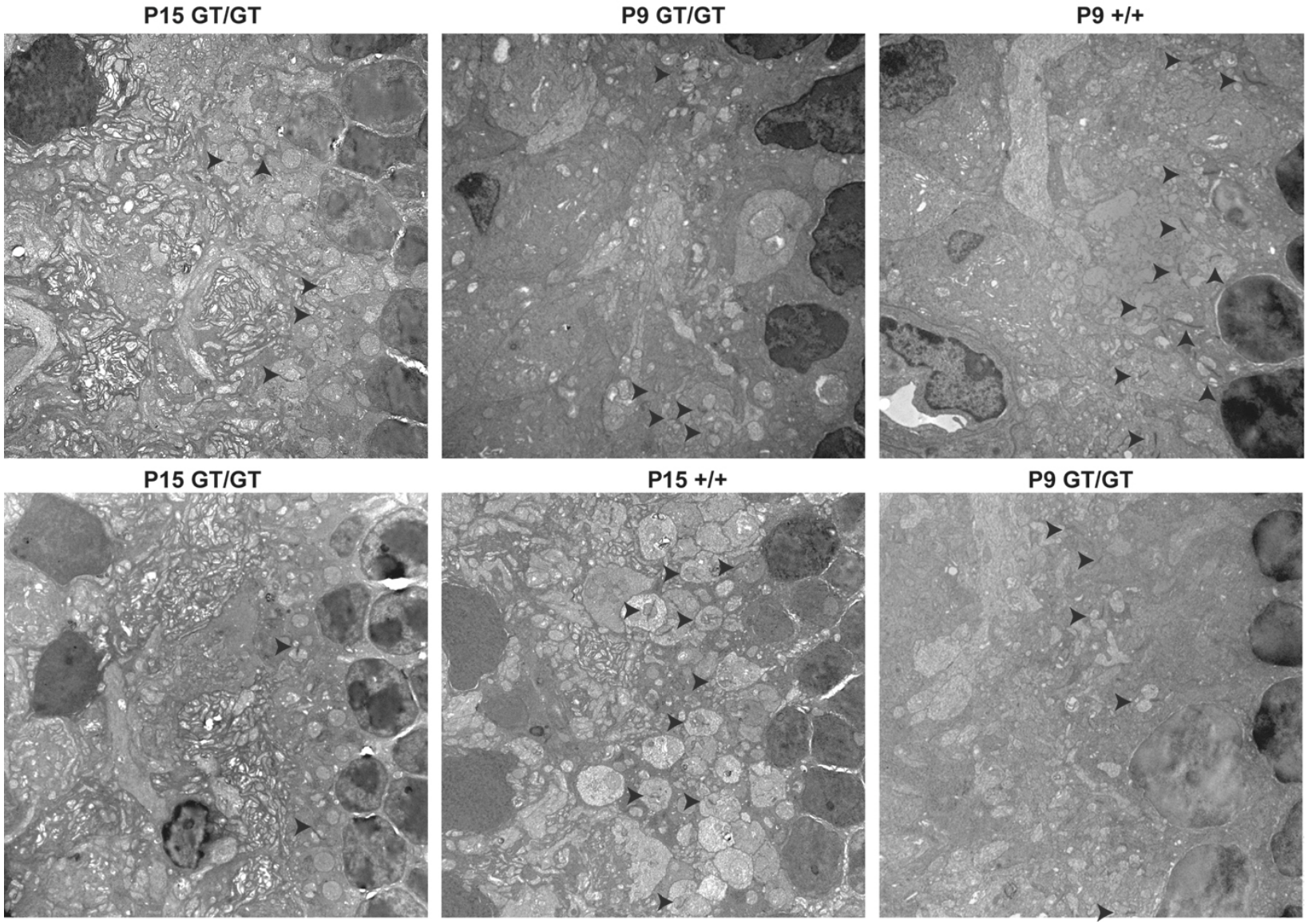
P15 GT/GT
P9 GT/GT
P9 +/+
P15 GT/GT
P15 +/+
P9 GT/GT

Supplemental 7. *Dscaml1* is not required for mosaic patterning of amacrine and RGC cell types that do not express it. Sections or whole retinas from wild type and *Dscaml1*$^{GT/GT}$ mice were stained with antibodies to ChAT, a marker of cholinergic amacrine cells (**A** and **B**); tyrosine hydroxylase (TH), a marker of dopaminergic amacrine cells (**C** and **D**); SMI-32, a marker of alpha retinal ganglion cells (**E** and **F**) and melanopsin, a marker of melanopsin-positive RGCs (**G** and **H**) (N≥3). No significant difference (as determined by DRP analysis) in the organization of cholinergic amacrine cells (**A** and **B**), dopaminergic amacrine cells (**C** and **D**), alpha retinal ganglion cells (**E** and **F**) or melanopsin positive retinal ganglion cells (**G** and **H**) were detected when comparing wild type and retinas. The scale bar below the lower right panel is equivalent to 387.5 μm.

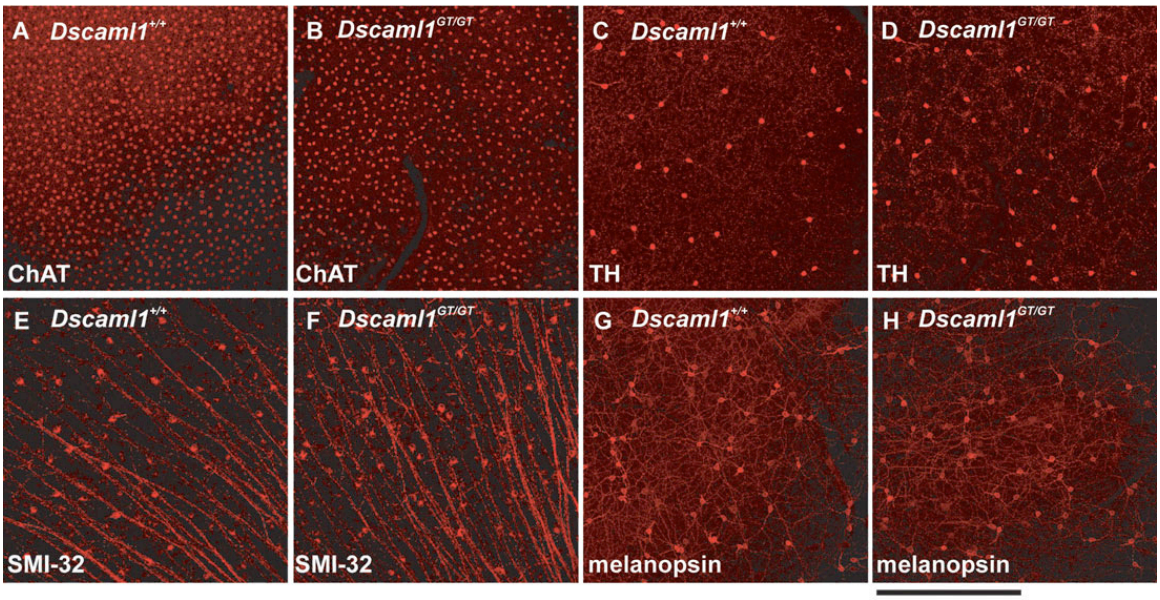

Supplemental Figure 8. Comparison of ERG amplitudes. No significant difference between wild type and *Dscaml1*$^{GT/GT}$ ERG amplitudes was detected. Significant differences were observed when comparing the A-wave of *Dscaml1*$^{GT/GT}$ and *Dscam*$^{-/-}$ mice and when comparing the B wave and combined A and B wave amplitudes of *Dscam*$^{-/-}$ mice with either *Dscaml1*$^{GT/GT}$ or wild type mice. The A-wave is the negative potential caused by activation of the photoreceptors, the B-wave is the positive potential caused by the synaptic activation of the rod bipolar cells. The total change in potential from the peak of the A-wave to the B-wave is also shown (amplitude). All values are mean ± standard deviation.

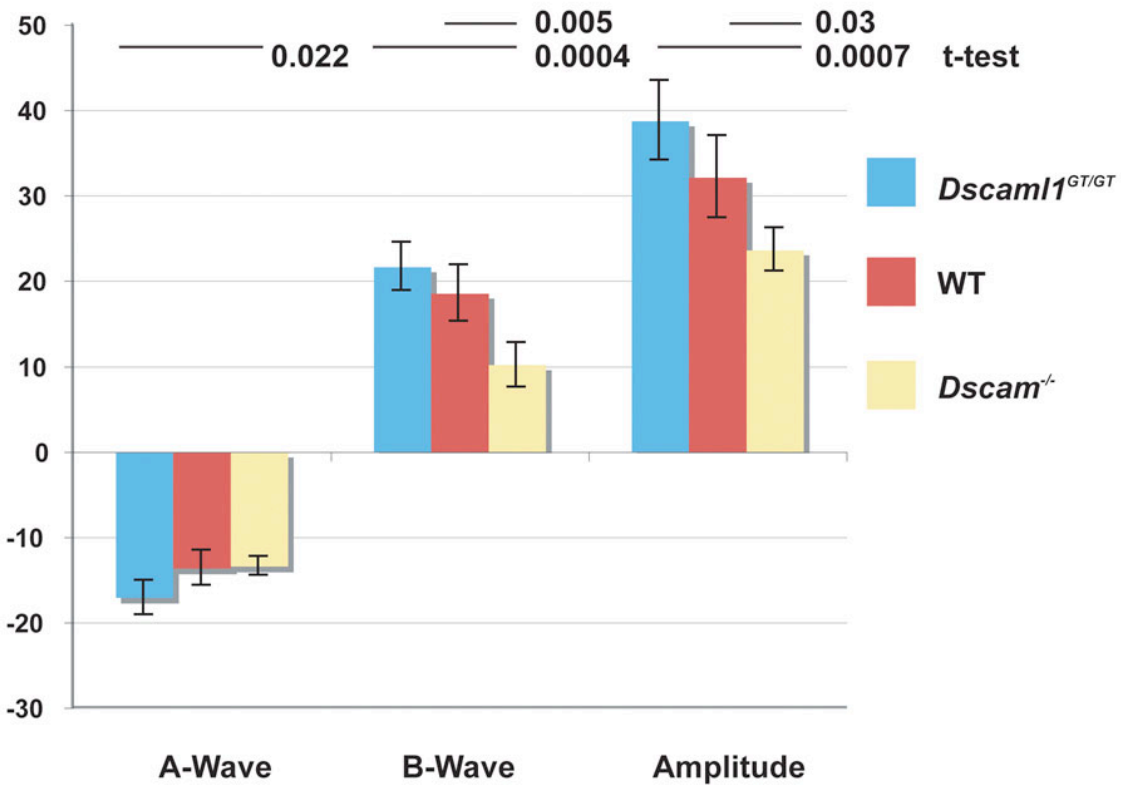

Supplemental Figure 9. Localization of PAK1 phosphoisoforms in wild type, *Dscam*$^{-/-}$ and *Dscaml1*$^{GT/GT}$ retinas. Sections of wild type, *Dscam*$^{-/-}$ and *Dscaml1*$^{GT/GT}$ retinas were stained with antibodies ChAT and one of the following phosphospecific PAK1 antibodies. PAK1S144^{P}, PAK1S199^{P}, PAK1T212^{P} and PAK1T423^{P}. No difference was detected when comparing wild type retinas to *Dscam*$^{-/-}$ or *Dscaml1*$^{GT/GT}$ retinas. The scale bar under the lower right panel is equivalent to 132 μm.

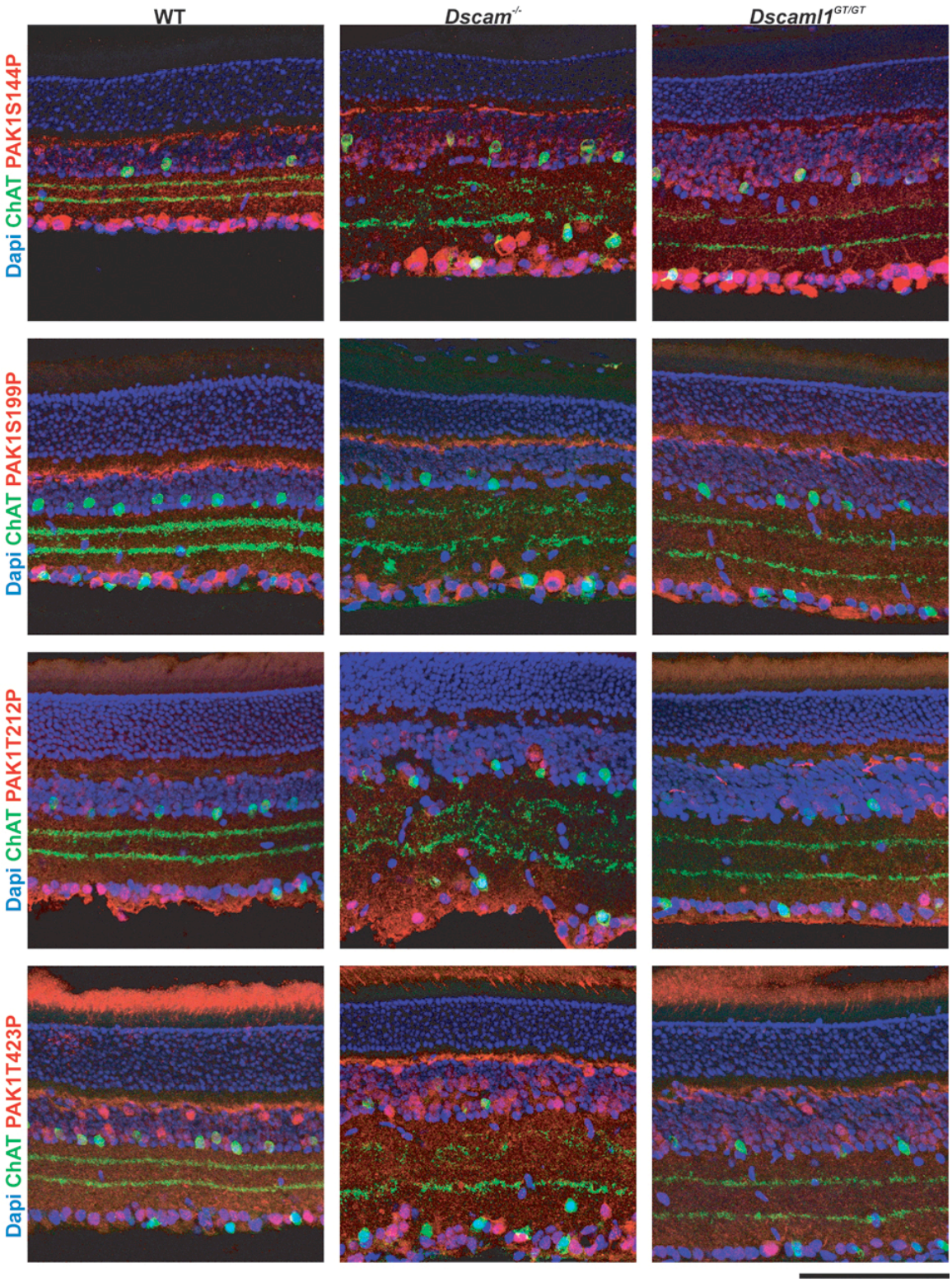
WT
Dscam-/-
Dscaml1GT/GT
Dapi ChAT PAK1S144P
Dapi ChAT PAK1S199P
Dapi ChAT PAK1T212P
Dapi ChAT PAK1T423P

Supplemental 10. RGC neurite fasciculation and soma aggregation precede delayed developmental cell death. **A**, The number of BRN3a-positive RGCs was counted in wild type, *Dscam*$^{+/-}$ retinas and *Dscam*$^{-/-}$ retinas (N≥3 per genotype per time point, values are mean ± standard error measure). No significant difference was observed at P0. A significant difference was found between wild type and both *Dscam* heterozygotes and homozygotes at P5. No significant difference in the number of RGCs was observed in the adult retina, although a significant increase in the number of RGCs was observed when comparing the peripheral *Dscam*$^{-/-}$ retina to the peripheral wild type retina. **B**, **C**, Wild type and *Dscam*$^{-/-}$ retinas, collected at P0, were stained with antibodies to melanopsin (N>3). Melanopsin-positive retinal ganglion cells are aggregated at P0 in the mutant retina (**C**) compared to wild type (**B**). **D**, **E**, Wild type and *Dscam*$^{-/-}$ retinas, carrying the Mito-Y transgene, were collected at P0. Mito-Y positive ganglion cells are aggregated at P0 in the mutant retina (**E**) compared to wild type (**D**) (N=3). **F**, **G**, Aggregation and fasciculation was not observed in *BAX* deficient retinas **(**N=4 at P0). The scale bar in (**I**) is equivalent to 349 μm in **B-E** and 386.5 μm in **F** and **G**.

Cell count methods

Neural retinas were dissected free of the lens and RPE, boiled for 10 min in 10 mM Sodium Citrate, pH 6.0 and left at room temp for 20 min to cool. Retinas were blocked with 10% NGS/0.2%BSA/0.1% Triton X-100/PBS + 0.02% sodium azide for 90 minutes and incubated for 2 days in anti-BRN3A (Millipore (UK) Ltd, Watford UK), washed with PBS and incubated overnight in AlexaFluor-488 goat anti-mouse IgG (Invitrogen Ltd, Paisley UK.; 1:250). Labeled retinas were mounted in Vectashield (Vector Labs) and

imaged using a Zeiss LSM 510 confocal microscope. Z-stacks through the entire depth of the BRN3A-positve regions of each retina were collected from 4 areas centered on the optic disc (1/retinal quadrant) and from corresponding regions located in the retinal periphery. The number of BRN3A-positive cells in each Z-stack was counted using Image J and the mean ± s.e.m cell density in the central, peripheral or whole retina calculated. A low power image of the entire retina was captured using a Nikon SMZ1500 stereomicroscope with a Nikon DXM1200 digital camera with ACT-1 software, the retinal area measured using Image J and the number of cells/retina determined.

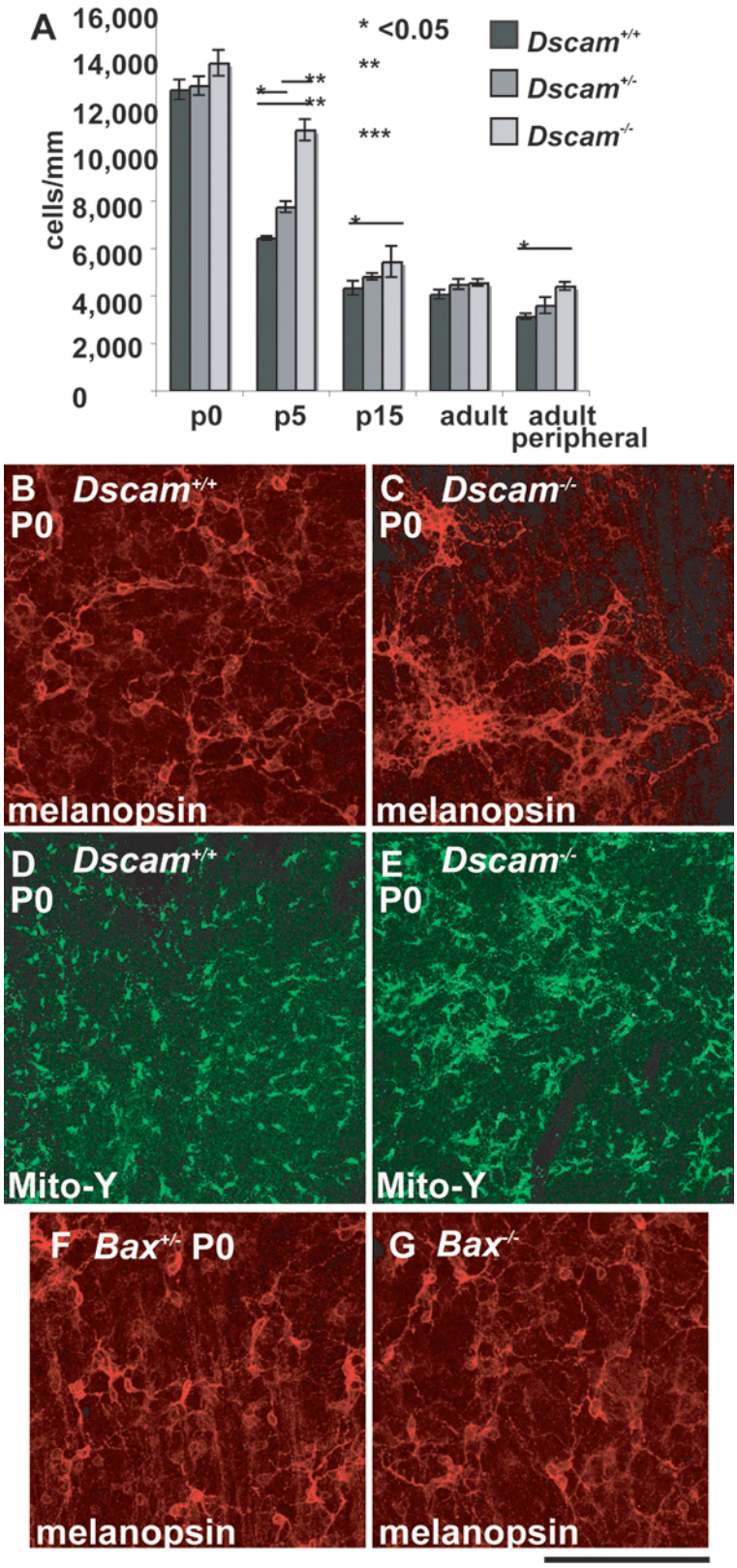
A
16,000
14,000
12,000
10,000
8,000
6,000
4,000
2,000
0
cells/mm
* <0.05
**
***
Dscam+/+
Dscam+/-
Dscam-/-
p0
p5
p15
adult
adult peripheral
B Dscam+/+ P0
melanopsin
C Dscam-/- P0
melanopsin
D Dscam+/+ P0
Mito-Y
E Dscam-/- P0
Mito-Y
F Bax+/- P0
melanopsin
G Bax-/-
melanopsin